

This discussion paper is/has been under review for the journal Atmospheric Chemistry and Physics (ACP). Please refer to the corresponding final paper in ACP if available.

**Size-dependent  
aerosol deposition  
velocities**

R. J. Vong et al.

# Size-dependent aerosol deposition velocities during BEARPEX'07

R. J. Vong<sup>1</sup>, I. J. Vong<sup>1</sup>, D. Vickers<sup>1</sup>, and D. S. Covert<sup>2</sup>

<sup>1</sup>College of Oceanic and Atmospheric Sciences, Oregon State University, Corvallis, OR, 97331 USA

<sup>2</sup>Joint Institute for the Study of Atmospheres and Oceans, University of Washington, Seattle, WA, USA

Received: 17 December 2009 – Accepted: 8 February 2010 – Published: 16 February 2010

Correspondence to: R. J. Vong (vong@coas.oregonstate.edu)

Published by Copernicus Publications on behalf of the European Geosciences Union.

Title Page

Abstract

Introduction

Conclusions

References

Tables

Figures

◀

▶

◀

▶

Back

Close

Full Screen / Esc

Printer-friendly Version

Interactive Discussion



## Abstract

Aerosol concentrations and 3-D winds were measured from 9 to 25 September 2007 above a pine forest in California. The measurements were combined using the eddy covariance (EC) technique to determine aerosol eddy fluxes as a function of particle diameter within the accumulation mode size range ( $0.25\ \mu\text{m} < \text{dia} < 1\ \mu\text{m}$  here). Measured heat and water vapor fluxes were utilized to correct the aerosol eddy fluxes for aerosol hygroscopic growth. The hygroscopic growth correction was necessary despite the low RH and relatively hydrophobic nature of the particles. Uncertainties associated with particle counting also were evaluated from the data. Aerosol deposition velocities ( $V_d = \text{EC turbulent flux}/\text{mean particle concentration}$ ) during daytime were shown to vary from  $-0.2$  to  $-1.0\ \text{cm s}^{-1}$ ;  $|V_d|$  increases with friction velocity and particle diameter.

## 1 Introduction

Removal of aerosol particles to vegetation by atmospheric turbulence is the focus of this experiment that addresses key factors which control the magnitude of aerosol flux and its uncertainties. These factors relate to aerosol microphysics, aerosol chemical composition, and boundary layer dynamics.

The concentration and chemical composition of atmospheric, accumulation mode ( $0.1\ \mu\text{m} < \text{dia} < 2.0\ \mu\text{m}$ ) aerosol are important influences on the Earth's climate, air quality, clouds, and precipitation (Charlson et al., 1987, 1992). The composition, concentration, and spatial distribution of aerosol are controlled by emission, transport and mixing, chemical and physical processing, and deposition. Aerosol removal via clouds and precipitation is known as wet deposition while removal by cloud-free, turbulence related processes (including impaction, interception and diffusion) and gravitational settling are termed dry deposition.

Dry deposition can contribute a substantial fraction (up to one-half) of the total chemical mass in atmospheric deposition (Erisman et al., 1997; Hicks et al., 1991) and can

### Size-dependent aerosol deposition velocities

R. J. Vong et al.

Title Page

Abstract

Introduction

Conclusions

References

Tables

Figures

◀

▶

◀

▶

Back

Close

Full Screen / Esc

Printer-friendly Version

Interactive Discussion



result in potentially significant impacts on terrestrial and aquatic ecosystems. However, rates and mechanisms for the removal of accumulation mode particles by turbulence are not well known nor is the dependence of particle deposition velocity ( $V_d$ ) on diameter (Pryor et al., 2008).

## 2 Methods

### 2.1 Site

Aerosol concentrations and winds were measured from 9 to 25 September 2007 above a pine forest owned by Sierra Pacific Industries, adjacent to the University of California at Berkeley's Blodgett Forest Research Station as part of the Biosphere Effects on Aerosols and Photochemistry Experiment (BEARPEX). The site is located 75 km NE of Sacramento, CA (38°59' N, 120° 58' W) at 1315 m. elevation on the western slope of the Sierra Nevada mountains. The area was planted with *Pinus ponderosa* in 1990 with a few other species present; average canopy height was 7.9 m. The understory is composed of manzanita and mountain whitehorn shrubs up to 2 m in height. The leaf area index for the full canopy was 5.1 m<sup>2</sup>/m<sup>2</sup>. A detailed description of the site is provided by Goldstein et al. (2000). The daytime fetch is excellent in that the upwind (winds from the SE to W) canopy is even aged and uniform over a distance of 2 km and the terrain is gently sloped (2°). The night time fetch (winds from the E and N) is not as good because of uneven upwind terrain and advection of emissions from the site's electrical generator (located ~125 m. to the N).

### 2.2 Instrumentation

Aerosol concentrations as a function of particle diameter were measured by light scattering techniques. The FAST aerosol spectrometer (Flux Aerosol Spectrometer Technique, Droplet Measurement Technologies, DMT Boulder CO) provided particle concentration at 10 Hz as a function of size for the eddy covariance (EC) fluxes while two

## Size-dependent aerosol deposition velocities

R. J. Vong et al.

Title Page

Abstract

Introduction

Conclusions

References

Tables

Figures

◀

▶

◀

▶

Back

Close

Full Screen / Esc

Printer-friendly Version

Interactive Discussion



identical optical particle counters (OPC, WELAS 2100, Palas, Karlsruhe, Germany) measured the aerosol size spectra and hygroscopic growth at 5 min resolution. The FAST and OPCs provided detailed resolution of the aerosol size spectrum for much of the accumulation mode size range ( $0.25 \mu\text{m} < \text{dia} < 1.0 \mu\text{m}$  here).

5 The FAST illuminates the aspirated aerosol particles with a 680 nm laser beam and detects the scattered light ( $5^\circ$  to  $14^\circ$  forward collection angle) (Vong et al., 2004). The FAST was size-calibrated using PSL particles and its counting efficiency was determined as a function of diameter by comparison to a second instrument (UHSAS, DMT Boulder CO) in the laboratory and to the OPCs in the field. The FAST undercounted the  
10 smaller particles ( $\text{dia} < 0.4 \mu\text{m}$ ) compared to the UHSAS and OPCs before correction. The FAST was operated continuously during daytime and some nights.

The two WELAS white-light OPCs were operated regularly but not continuously each day to quantify aerosol hygroscopic growth during the morning, afternoon and early evening hours. Water vapor was added to and removed from the sample air upstream  
15 of the two OPCs to achieve relative humidities (RH) that bracketed the ambient RH in order to determine the hygroscopic growth parameter ( $\gamma$ ) relevant for the FAST measurement. The OPCs were located inside a sampling van at the base of the tower and drew air at 12 l/m through a common 1/2 cm diameter conductive polyethylene tube from the 18.8 m a.g.l. tower level near the EC instrumentation. The OPCs were size  
20 calibrated with PSL particles of 250 to 900 nm. Their counting efficiency was determined by comparison to condensation particle counters (Model 3010, TSI, St. Paul MN) using PSL selected by a differential mobility analyzer (Model 3071, TSI).

Water vapor was measured in situ at 10 Hz by ultraviolet absorption (Model KH-20  
25 Campbell Scientific, Logan UT), three dimensional winds and virtual temperature at 10 Hz using an ultrasonic anemometer (Model SWS-211-3K Appl. Tech. Inc., Boulder CO), and temperature and RH (Model HMP-45C Campbell Scientific, Logan UT) gradients were measured at 30 min intervals (at 18.8 m/7.3 m a.g.l.).

The EC technique combined aerosol concentrations from the FAST, water vapor density from the KH-20, and 3-D winds from the sonic anemometer as calculated covari-

---

**Size-dependent  
aerosol deposition  
velocities**R. J. Vong et al.

---

[Title Page](#)[Abstract](#)[Introduction](#)[Conclusions](#)[References](#)[Tables](#)[Figures](#)[◀](#)[▶](#)[◀](#)[▶](#)[Back](#)[Close](#)[Full Screen / Esc](#)[Printer-friendly Version](#)[Interactive Discussion](#)

ances; all of these measurements were performed from the top of a scaffolding tower at 18.8 m a.g.l. The EC instruments were mounted on a boom that extended 2 m upwind of the SW tower corner in order to minimize flow distortion from the scaffolding. The boom and instruments were periodically oriented (generally 2 to 3 times per day) into the prevailing wind direction by rotating the boom. Inlet nozzles of varying diameter matched the FAST aspiration velocity to ambient wind speed to achieve isokinetic sampling.

### 2.3 Data processing for aerosol EC fluxes

The eddy covariance (EC) fluxes for the FAST were determined after combining the particle concentrations from its twenty aerosol size intervals into six broader size intervals to obtain more total counts for each diameter interval within each 30 min flux period. These six aerosol sizes covered the range  $0.25 \mu\text{m} < \text{dia} < 1.0 \mu\text{m}$ . Thus, aerosol concentrations and fluxes were determined separately from the FAST for the diameters listed in Table 1.

In a 0.1 s sampling interval, the FAST typically counted 1 to 10 particles in the larger diameter ( $\text{dia} \geq 0.5 \mu\text{m}$ ) intervals but 5 to 40 particles in the for the smaller (e.g.,  $0.3 \mu\text{m}$ ) particles. For any 30 min eddy flux during BEARPEX, the total particle counts in any diameter interval varied from  $\sim 10^4$  to  $2 \times 10^5$ .

Periods with at least 28 (of 30) min of valid data were retained for further analysis. Data were deemed valid after screening for periods with signal dropouts, activity on the tower, sonic anemometer or hygrometer spikes during rain, boom rotation, and poor upwind fetch. To avoid these problems as well as the result of applying standard micrometeorological screening of eddy flux data (Vickers and Mahrt, 1997; Vickers and Mahrt, 2003) the data set was reduced to its most ideal periods: 316 total 30-min periods with valid aerosol eddy fluxes (most were daytime hours) with 67 of these periods also having aerosol hygroscopic growth measurements (twice each day).

After the above data screening steps, tilt and coordinate system rotations were investigated (Lee et al., 2004). The derived rotation (“attack”) angle ( $2^\circ$  mean) matched

## Size-dependent aerosol deposition velocities

R. J. Vong et al.

Title Page

Abstract

Introduction

Conclusions

References

Tables

Figures

◀

▶

◀

▶

Back

Close

Full Screen / Esc

Printer-friendly Version

Interactive Discussion



---

**Size-dependent  
aerosol deposition  
velocities**R. J. Vong et al.

---

[Title Page](#)[Abstract](#)[Introduction](#)[Conclusions](#)[References](#)[Tables](#)[Figures](#)[◀](#)[▶](#)[◀](#)[▶](#)[Back](#)[Close](#)[Full Screen / Esc](#)[Printer-friendly Version](#)[Interactive Discussion](#)

the slope of the upwind terrain such that vertical fluxes were both “surface normal” and streamline normal. This attack angle derived from the daytime BEARPEX data resulted in similar EC fluxes whether rotations were derived from data for each 30 min flux period or alternatively based on mean “attack angle” as a function of wind direction (Kowalski et al., 1997). These different rotation criteria also produced similar values for friction velocity ( $u^*$ ) indicating that the fluxes are not sensitive to the rotation criteria at this site.

The eddy covariance heat, vapor, and momentum fluxes that are reported here showed good agreement with those measured independently by Univ. of California collaborators for the same time periods (regression slopes were 0.96 to 1.1;  $r^2 = 0.77$  to 0.92) despite the fact that their fluxes were measured from a second tower that was located 12 m away (cross wind) and at a lower height (13 m a.g.l. for U.C. vs. 18.8 m here). This type of consistency between fluxes measured at different heights and cross wind locations suggests that these EC measurements are representative of the upwind fetch.

### 3 Results

#### 3.1 General

The winds were predictable with upslope winds (S to W) over good fetch from late morning until sundown each day but down slope winds (N to E) at night and early morning. Concentrations were quite low except for a few periods when forest fires elevated particle and gas concentrations. The ambient relative humidity was in the range  $15\% < RH < 40\%$  during most daytime periods.

#### 3.2 Eddy covariance fluxes

Figure 1 presents the measured diurnal variation of aerosol deposition velocity ( $V_d = EC \text{ turbulent flux} / \text{mean particle concentration}$ ) during BEARPEX. Deposition ve-

**Size-dependent  
aerosol deposition  
velocities**

R. J. Vong et al.

Title Page

Abstract

Introduction

Conclusions

References

Tables

Figures

◀

▶

◀

▶

Back

Close

Full Screen / Esc

Printer-friendly Version

Interactive Discussion



locities are presented to characterize the aerosol turbulent fluxes to remove both the dependence of flux on concentration and the counting efficiency correction. Aerosol fluxes and  $|V_d|$  were larger during mid-afternoon than mornings or evenings. Analysis of daytime sonic anemometer data indicates that the turbulence at the measurement height is fully developed (Stull, 1988; Foken et al., 2004) in that the expected relationship exists among vertical and horizontal turbulent wind components ( $\sigma_w = 1.33 u^*$  with  $r^2=0.93$ , where  $\sigma_w$  is the standard deviation of the vertical wind component and  $u^*$  is the friction velocity, both over 30 min).

### 3.3 Counting uncertainties

The uncertainty for single 30-min EC aerosol fluxes due to the discrete nature of aerosol “counting” was calculated as  $\sigma_w/\sqrt{N}$  (Fairall, 1984; Nemitz et al., 2002; Vong et al., 2004) where  $N$  is the number of particles counted in 30 min for a particular particle size. Counting uncertainties, in terms of the particle deposition velocity, were  $\pm 0.14$  to  $0.21$  cm/s for the smaller particles ( $0.25 \mu\text{m} < \text{dia} < 0.44 \mu\text{m}$ ) but were  $\pm 0.55$  cm/s for the larger particles ( $0.5 \mu\text{m} < \text{dia} < 1.0 \mu\text{m}$ ) for single 30-min EC aerosol flux periods. The uncertainty in the pooled values for mean deposition velocity ( $V_d$ ) during BEARPEX would be  $1/\sqrt{316}$ , or 6%, of these values. These uncertainties are acceptable for the smaller ( $\text{dia} < 0.5 \mu\text{m}$ ) particles but large enough to reduce confidence in the results for the larger ( $\text{dia} > 0.5 \mu\text{m}$ ) particles.

### 3.4 Spectra and co-spectra

Figure 2 presents BEARPEX aerosol frequency spectra from the FAST spectrometer, spectra of vertical velocity, water vapor density, and virtual temperature, their co-spectra, and the  $[-5/3]$  spectral slope that would be expected for an instrument with an ideal response. While vertical velocity, water vapor, and virtual temperature behave as expected, aerosol concentration for all six particle diameters does not. The flattening of particle concentration variance in the spectrum suggests that noise is present and

that the FAST did not resolve aerosol concentration at the higher frequencies.

There is no appreciable difference between the particle spectra for six different diameters in that they each flatten out at frequencies above ca.  $2 \times 10^{-1}$  Hz (Fig. 2, top panel). The FAST signals are dominated by white noise for anything faster than 5 s resolution. These spectra for heat, water vapor, and vertical wind follow the  $[-5/3]$  theoretical slope suggesting that these quantities are well determined out to 5 Hz (Fig. 2, middle panel). The effect of averaging time on the computation of EC fluxes was found to be minimal in that 10-min or 30-min mean removal made only 1–2% difference in the 30 min fluxes.

The bottom panel in Fig. 2 presents cospectra as the cumulative, normalized, covariance for heat, water vapor, particles (0.3  $\mu\text{m}$  diameter is displayed; other particle diameters behave similarly), and momentum. The particle flux occurs over the same frequency ranges as heat, moisture, and momentum fluxes for  $f < 5 \times 10^{-1}$  (i.e., 0.5 Hz). The heat and vapor turbulent fluxes have a 12 to 16% contribution to their total fluxes above 0.2 Hz while the particle fluxes have a similar contribution (15.6% of the measured covariance for 0.3  $\mu\text{m}$  diameter particles). Above 0.5 Hz the particle cospectrum falls to near zero whereas the heat and vapor fluxes still contribute 6–9% of the total covariance. From this it appears that the lack of frequency response by the FAST results in a loss of at least 6–9% of the aerosol EC flux and as much as 16% could have been lost due to its inability to resolve high frequencies. The smaller error estimate is based on the amount of vapor and heat flux above 0.5 Hz (where the particle covariance becomes small) whereas the larger estimate assumes that the FAST lost all flux above 0.2 Hz (where the spectrum becomes white).

Most of the aerosol flux is transported over time scales of 2 to 200 s while the heat, vapor and momentum fluxes, according to the cospectra, are transported by slightly larger eddies with time scales of 2 to 500 s. Although it is clear that the FAST is not an ideal EC scalar sensor based on the co-spectra, it did capture covariance in the same frequency ranges that dominated the other turbulent fluxes. After applying a low-pass noise filter with a cutoff frequency of 0.5 Hz (half power of the filter) the spectra follow

**Size-dependent  
aerosol deposition  
velocities**

R. J. Vong et al.

Title Page

Abstract

Introduction

Conclusions

References

Tables

Figures



Back

Close

Full Screen / Esc

Printer-friendly Version

Interactive Discussion



the  $[-5/3]$  slope in the inertial sub-range. The scale dependence of the flux is nearly the same for the unfiltered and filtered time series, indicating that the high-frequency noise does not contribute significantly to the eddy flux.

The particle fluxes would be attenuated at the higher frequencies (Moore, 1986) due to the 0.9 m lateral separation of the FAST from the sonic anemometer but these corrections are not important here because the aerosol spectrometer does not resolve these frequencies (Fig. 2, top panel) and very little of the observed particle flux occurs at these time scales (Fig. 2, bottom panel).

### 3.5 Aerosol hygroscopic growth

The FAST, by necessity, operates at ambient RH. Since RH can vary rapidly in time due to upward and downward transport of parcels from layers with higher or lower humidity, and because ambient aerosol is hygroscopic in varying degrees, a given aerosol number-size distribution will vary with changing RH and affect the EC fluxes from the FAST. Even if the hygroscopic growth factor is small, the effect on EC fluxes can be large if the slope of the distribution is steep in the range covered by the FAST. For a typical accumulation mode number-size distribution with a steep negative slope, the FAST will report a larger concentration at a given size increment within a higher RH parcel compared to that measured at a lower RH due to the hygroscopic growth-size shift in the distribution. The converse will occur with lower RH parcels. Thus, a hygroscopic growth measurement and correction is needed for this EC flux measurement. Hygroscopic growth is determined by the chemical composition of the aerosol and does not vary rapidly in time under conditions that are required for flux measurements.

The hygroscopic aerosol growth parameter,  $\gamma$ , was calculated twice daily from aerosol size spectra measured by OPCs operating at different RH. Equation (1) (Kasten, 1969; Vong et al., 2004; Massling et al., 2005) relates the measured diameters to yield the hygroscopic growth parameter ( $\gamma$ ) as

$$D(S_{\text{high}})/D(S_{\text{low}})=[(1 - S_{\text{high}})/(1 - S_{\text{low}})]^{-\gamma} \quad (1)$$

## Size-dependent aerosol deposition velocities

R. J. Vong et al.

Title Page

Abstract

Introduction

Conclusions

References

Tables

Figures

◀

▶

◀

▶

Back

Close

Full Screen / Esc

Printer-friendly Version

Interactive Discussion



where:  $S$  is saturation ratio ( $S = RH/100\%$ ),  $S_{low}$  and  $S_{high}$  describe the high and low RH values during OPC scans,  $D$  is aerosol optical diameter at the given saturation ratio ( $S = RH/100\%$ )

### 3.6 Hygroscopic growth correction to aerosol deposition velocity

5 A correction to aerosol EC fluxes, in terms of deposition velocity, due to any hygroscopic growth of particles is given as (Vong et al., 2004; Kowalski, 2001; Fairall, 1984):

$$\Delta V_d = -\beta \gamma \overline{w' S'} / (1 - S) \quad (2)$$

All the components of this  $V_d$  correction were measured during BEAREPX 2007: the slope of the aerosol number-size distribution ( $\beta$ ), the hygroscopic growth parameter ( $\gamma$ ), the saturation ratio, and the saturation ratio flux ( $\overline{w' S'}$ ).

10 During BEARPEX the hygroscopic growth parameter was measured to be in the range  $0 < \gamma < 0.12$  based on 258 valid scans with a mean value of  $\gamma = 0.06$  over the optical size range of 0.3 to 1.0  $\mu\text{m}$ . There was no difference in measured  $\gamma$  with diameter and no trend with time during BEARPEX. Figure 3 displays the variation in the exponent for Eq. (1) (presented as  $-\gamma$ ) and a Gaussian fit to its frequency distribution.

15 This small value of  $\gamma$  during BEARPEX compares to  $\gamma = 0.25$  for pure ammonium sulfate aerosol (Vong et al., 2004). Thus, the BEARPEX aerosol were much less hygroscopic than sulfate or other inorganic, combustion-derived particulate chemistry. For humidity changes from low RH ( $RH \leq 30\%$ ) to 90% RH, the typical BEARPEX aerosol grew by a factor of 1.12 in diameter while sulfate particles would grow by a factor of 1.78. These results are consistent with previous measurements of hygroscopic growth of aerosol in the California Sierra Nevada region where Carrico et al. (2005) measured particle growth by factors of 1.11 and 1.29 for two observed modes of the aerosol (for 0.2  $\mu\text{m}$  diameter at high RH).

25 The aerosol size distribution during BEARPEX, characterized by the “Junge” slope ( $\beta$ : as defined as  $dN/d\log D = cD^{-\beta}$ ) was calculated for every 30 min flux interval for

## Size-dependent aerosol deposition velocities

R. J. Vong et al.

Title Page

Abstract

Introduction

Conclusions

References

Tables

Figures

◀

▶

◀

▶

Back

Close

Full Screen / Esc

Printer-friendly Version

Interactive Discussion



each FAST diameter interval and shown to be “very steep” ( $4 < \beta < 10$ ).  $\beta$  decreased with increasing particle diameter. Because of these steep slopes there were high concentrations of smaller particles that could grow into a given FAST diameter interval in higher RH air parcels arriving at the FAST during vertical transport. Similarly, there were few larger particles that could shrink into a given diameter interval when RH decreased during vertical transport. Figure 4 presents the average aerosol size distribution from the OPCs.

The saturation ratio flux is defined as (Kowalski 2001; Fairall, 1983):

$$\overline{w'S'} = \overline{w'q'}/q_{\text{sat}} - \overline{w'T'}(SL_v)/(R_vT^2) \quad (3)$$

This saturation ratio flux was determined from measured 10 Hz heat and vapor EC fluxes according to Eq. (3) and was similar to values observed over grass in Oregon during EFLAT by Vong et al. (2004). Positive  $\overline{w'S'}$  were observed at night and negative values were observed during the day (Fig. 5).

During the daytime, measured aerosol deposition velocities change by becoming less downward after a hygroscopic growth correction. This hygroscopic behavior of the particles reflected the fact that RH was 1 to 6% higher at the top of the tower (at 18.8 m a.g.l.) than below (at 7.3 m a.g.l.) during daytime making saturation ratio flux  $\overline{w'S'}$  downward (negative). At night or during the early morning periods when RH was 5 to 15% higher near the ground than at the top of the tower, the measured aerosol deposition velocities change by a smaller amount and become more downward after a hygroscopic growth correction. The hygroscopic growth correction during BEARPEX reduces the magnitude of both upward and downward aerosol eddy fluxes and deposition velocities compared to observed, uncorrected values.

Figure 6 displays the measured and hygroscopic growth-corrected aerosol deposition velocities for six aerosol diameters particles plotted against friction velocity ( $u^*$ ) to demonstrate the magnitude of the correction. In these plots, the uncertainties represent  $\pm$  one data standard error of the measured values among the 188, 30-min observations that are included for each diameter.

## Size-dependent aerosol deposition velocities

R. J. Vong et al.

Title Page

Abstract

Introduction

Conclusions

References

Tables

Figures

◀

▶

◀

▶

Back

Close

Full Screen / Esc

Printer-friendly Version

Interactive Discussion



### 3.7 WPL corrections

Webb-Pearman-Leuning (WPL) corrections (Webb et al., 1980) were performed to determine how the aerosol deposition velocity was affected by vertical variations in air density (associated with  $T$  and RH gradients) according to Eq. (4):

$$V_d = 1.61 \overline{(w' \rho_{H_2O}' / \rho_{air})} + (1 + 1.61 q) \overline{(w' T' / T)} \quad (4)$$

The Webb correction reached maximum values of 0.05 to 0.15 cm/s during the middle of each day (10 a.m. until 3 p.m.) and was negligible (less than  $\pm 0.02$  cm/s) in the mornings and evenings. These corrections are incorporated in the results presented in Fig. 6 and 7. However, the aerosol fluxes depended on moisture variations more through the hygroscopic growth corrections than on WPL corrections.

### 3.8 Dependence on friction velocity

Both the transport of particles by turbulence through the atmospheric surface layer and their subsequent removal by inertial impaction ought to depend on friction velocity (Pryor et al., 2008; Gallagher et al., 1997). As shown in Fig. 6, aerosol deposition velocity was larger in magnitude for higher values of friction velocity ( $u^*$ ), i.e.  $V_d$  becomes more negative. Negative fluxes and negative  $V_d$  imply downward transfer here (towards the ground, consistent with the sign convention for vertical velocity,  $w$ ).

### 3.9 Size-dependence of deposition velocity

Particle inertial impaction ought to depend on diameter because larger particles have more momentum. Thus, the removal of accumulation mode particles onto a forest canopy and the resulting aerosol  $|V_d|$  ought to increase with both  $u^*$  and particle diameter. Figure 7 shows that  $|V_d|$  during BEARPEX increased with particle size for the smaller accumulation mode aerosol ( $0.25 < \text{dia} < 0.4 \mu\text{m}$ ) during both low and high friction velocity time periods; in this figure the plotted errors bars represent the average counting error at that diameter for a single 30 min flux.

## Size-dependent aerosol deposition velocities

R. J. Vong et al.

Title Page

Abstract

Introduction

Conclusions

References

Tables

Figures

◀

▶

◀

▶

Back

Close

Full Screen / Esc

Printer-friendly Version

Interactive Discussion



The apparent decrease in the measured values of  $|V_d|$  for diameters greater than  $0.5\ \mu\text{m}$  is considered less reliable due to the larger counting uncertainties. The uncertainty in the mean values for deposition velocity in Fig. 7 are actually 8% ( $1/\sqrt{158}$ ) of those for single 30 min fluxes but the presentation of counting errors for single 30 min fluxes was chosen here because it highlights the fact that the results for larger diameters are much less reliable.

## 4 Discussion

When the low daytime RH were first observed at the Blodgett Forest site, it was expected that the hygroscopic growth correction might be small due to the combination of low daytime RH and the expected hydrophobic nature of aerosol composition in the area (Carrico et al., 2005). For the BEARPEX 2007 data, the steepness of the Junge slope of the number-size distribution offset the effect of small hygroscopic growth. The saturation ratio flux  $\overline{w'S'}$  during BEARPEX was similar to values reported for EFLAT (Vong et al., 2004) and HAPEX (Kowalski, 2001). Saturation ratio flux determined the sign of this hygroscopic growth correction but the slope of the aerosol size distribution and the hygroscopic growth parameter generally controlled its magnitude. It is likely that larger vertical velocity fluctuations over the “rougher” Blodgett Forest canopy compared to short grass in EFLAT resulted in better moisture vertical transport for a given RH gradient. Although the hygroscopic growth correction was moderate compared to the earlier EFLAT experiment in Oregon, it was important to the precise determination of aerosol deposition velocity at any diameter during BEARPEX.

There were too few stable cases sampled with good fetch during BEARPEX 2007 to characterize the relationship of aerosol  $V_d$  to atmospheric stability. The maximum  $|V_d|$  occurred during windy (high  $u^*$ ) afternoon conditions.

The apparent decrease in magnitude of aerosol  $V_d$  for diameters greater than  $0.4\ \mu\text{m}$  during BEARPEX likely reflects the fact that these fluxes are especially noisy due to higher counting errors. We consider that the size dependence of  $V_d$  for  $\text{dia} \leq 0.4\ \mu\text{m}$  is

### Size-dependent aerosol deposition velocities

R. J. Vong et al.

Title Page

Abstract

Introduction

Conclusions

References

Tables

Figures

◀

▶

◀

▶

Back

Close

Full Screen / Esc

Printer-friendly Version

Interactive Discussion



correctly characterized here but that values for the larger particles are more uncertain. These BEARPEX results for particle  $V_d$  are similar to those from studies that were conducted by Gallagher et al. (1997) in terms of the dependence of deposition velocity on friction velocity ( $u^*$ ) and the magnitudes of aerosol  $V_d$ ; both are larger than values predicted from the Slinn (1982) model.

## 5 Conclusions

Aerosol deposition velocity ( $V_d$ ) varied from  $-0.2$  to  $-1.0$   $\text{cm s}^{-1}$  during daytime as a function of both diameter and friction velocity ( $u^*$ ) for particle diameters from  $0.25$   $\mu\text{m}$  to  $0.4$   $\mu\text{m}$ . A hygroscopic growth correction to  $V_d$  was necessary for accurate results despite the low RH and relatively hydrophobic nature of the particles. The lack of high frequency response above  $0.2$  Hz by the EC aerosol sensor, the FAST, did not substantially affect the measured fluxes because most of the turbulent fluxes were transported by larger (lower frequency) eddies. Uncertainties associated with particle counting also were evaluated from the data and found to be substantial for particle diameters from  $0.4$   $\mu\text{m}$  to  $1$   $\mu\text{m}$ .

## References

- Carrico, C. M., Kreidenweis, S. M., Malm, W. C., Day, D. E. Lee, T., Carrillo, J., McMeeking, G. R., and Collett, J. L., Hygroscopic growth behavior of a carbon-dominated aerosol in Yosemite National Park, *Atmos. Environ.*, 39, 1393–1404, 2005.
- Charlson, R. J., Schwartz, S. E., Hales, J. M., Cess, R. D., Coakley, J. A., Hansen, J. E., and Hofmann, D. J., Climate forcing by anthropogenic aerosols, *Science* 255, 423–430, 1992.
- Charlson, R. J., Lovelock, J. E., Andreae, M. O., and Warren, S. G.: Oceanic phytoplankton, atmospheric sulfur, cloud albedo, and climate, *Nature*, 326, 655–661, 1987.
- Erismann, J. W., Draaijers, G., Duyzer, J., Hofschreuder, P., VanLeeuwen, N. et al.: Particle deposition to forests-summary of results and application, *Atmos. Environ.* 31, 321–332, 1997.

### Size-dependent aerosol deposition velocities

R. J. Vong et al.

Title Page

Abstract

Introduction

Conclusions

References

Tables

Figures

◀

▶

◀

▶

Back

Close

Full Screen / Esc

Printer-friendly Version

Interactive Discussion



**Size-dependent  
aerosol deposition  
velocities**

R. J. Vong et al.

[Title Page](#)[Abstract](#)[Introduction](#)[Conclusions](#)[References](#)[Tables](#)[Figures](#)[◀](#)[▶](#)[◀](#)[▶](#)[Back](#)[Close](#)[Full Screen / Esc](#)[Printer-friendly Version](#)[Interactive Discussion](#)

- Fairall, C. W.: Interpretation of eddy correlation measurements of particulate dry deposition, *Atmos. Environ.*, 18, 3129–3137, 1984.
- Foken, T., Gockede, M., Mauder, M., Mahrt, L., Amiro, B., and Munger, W.: Handbook of Micrometeorology, edited by: Lee, X., Massman, W. and Law, B., Kluwer Academic Press, Dordrecht, The Netherlands, 181–208, 2004.
- Gallagher, M. W., Beswick, K. M., Duyzer, J., Westrate, H., Choularton, T. W., and Hullmelshoj, P.: Measurements of aerosol fluxes to Speulder Forest using a micrometeorological technique, *Atmos. Environ.*, 31, 359–373, 1997.
- Goldstein, A. H., Hultman, N. E., Fracheboud, J. M., Bauer, M. R., Panek, J. A., Xu, M., Qi, Y., Guenther, A. B., and Baugh, W.: Effects of climate variability on the carbon dioxide, water, and sensible heat fluxes above a ponderosa pine plantation in the Sierra Nevada (CA), *Agr. Forest Meteorol.*, 101, 113–129, 2000.
- Hicks, B. B., Draxler, R. R., Albritton, D. L., Fehsenfeld, F. C., Dodge, M. C., Schwartz, S. E., Tanner, R. L., Hales, J. M., Meyers, T. P., and Vong, R. J.: Atmospheric Processes Research and Process Model Development, State-of-Science /Technology Report Number 2, National Acidic Precipitation Assessment Program (NAPAP), Washington DC, USA, 1991.
- Kasten, F.: Visibility forecast in the phase of pre-condensation, *Tellus*, 21, 631–635, 1969.
- Kowalski, A. S.: Deliquescence induces eddy covariance and estimable dry deposition errors, *Atmos Environ.* 35, 4843–4851, 2001.
- Kowalski, A. S., Anthoni, P. A., Vong, R. J., Delany, A. S., and Maclean, G.: Deployment and evaluation of a system for ground-based measurement of cloud liquid water fluxes, *J. Atmos. Ocean. Tech.* 14, 468–479, 1997.
- Lee, X., Finnigan, J., and Paw U, K. T.: Coordinate systems and flux bias error, in: Handbook of Micrometeorology, edited by: Lee, X., Massman, W., and Law, B., Kluwer Academic Press, Dordrecht, The Netherlands, 33–66, 2004.
- Massling, A., Stock, M., and Wiedensohler, A.: Diurnal, weekly, and seasonal variation of hygroscopic properties of submicrometer urban aerosol particles, *Atmos. Environ.*, 39, 3911–3922, 2005.
- Moore, C. J.: Frequency response corrections for eddy correlation systems, *Bound. Layer Meteorol.* 37, 17–35, 1986.
- Nemitz, E., Gallagher, M. W., Duyzer, J. H., and Fowler, D.: Micrometeorological measurements of particle deposition velocities to moorland vegetation, *Q. J. Roy. Meteor. Soc.*, 128, 2281–2300, 2002.



- Pryor, S. Gallagher, M. W., Sievering, H., Larsen, S. E., Barthemie, R. J., Birsan, F., Nemtizi, E., Rinne, J., Kulmala, M., Gronholm, T., Taipale, R., and Vesala, T., A review of measurement and modeling results of particle atmosphere-surface exchange, *Tellus 60B*, 42–75, 2008.
- 5 Slinn, W. G. N.: Predictions for particle deposition to vegetative canopies, *Atmos. Environ.*, 16, 1785–1794, 1982.
- Vickers, D. and Mahrt, L.: Quality control and flux sampling problems for tower and aircraft data, *J. Atmos. Ocean. Technol.*, 14, 512–526, 1997.
- Vickers, D. and Mahrt, L.: The cospectral gap and turbulent flux calculations, *J. Atmos. Ocean. Technol.*, 20, 660–672, 2003.
- 10 Vong, R. J., Vickers, D., and Covert, D. S.: Eddy correlation measurements of aerosol deposition to grass, *Tellus 56B*, 105–117, 2004.
- Webb, E. K., Pearman, G. I., and Leuning, R.: Correction of flux measurements for density effects due to heat and vapor transfer, *Q. J. Roy. Meteor. Soc.*, 106, 85–100, 1980.

---

**Size-dependent  
aerosol deposition  
velocities**R. J. Vong et al.

---

[Title Page](#)[Abstract](#)[Introduction](#)[Conclusions](#)[References](#)[Tables](#)[Figures](#)[I◀](#)[▶I](#)[◀](#)[▶](#)[Back](#)[Close](#)[Full Screen / Esc](#)[Printer-friendly Version](#)[Interactive Discussion](#)

**Size-dependent  
aerosol deposition  
velocities**

R. J. Vong et al.

**Table 1.** FAST sensing diameter range, intervals and mid-points.

FAST channel	Diameter interval, $\mu\text{m}$	Mid-point diameter, $\mu\text{m}$
A	0.246 to 0.280	0.26
B	0.28 to 0.31	0.30
C	0.31 to 0.34	0.33
D	0.34 to 0.44	0.40
E	0.44 to 0.54	0.49
F	0.54 to 1.01	0.78

[Title Page](#)[Abstract](#)[Introduction](#)[Conclusions](#)[References](#)[Tables](#)[Figures](#)[I◀](#)[▶I](#)[◀](#)[▶](#)[Back](#)[Close](#)[Full Screen / Esc](#)[Printer-friendly Version](#)[Interactive Discussion](#)

Size-dependent  
aerosol deposition  
velocities

R. J. Vong et al.

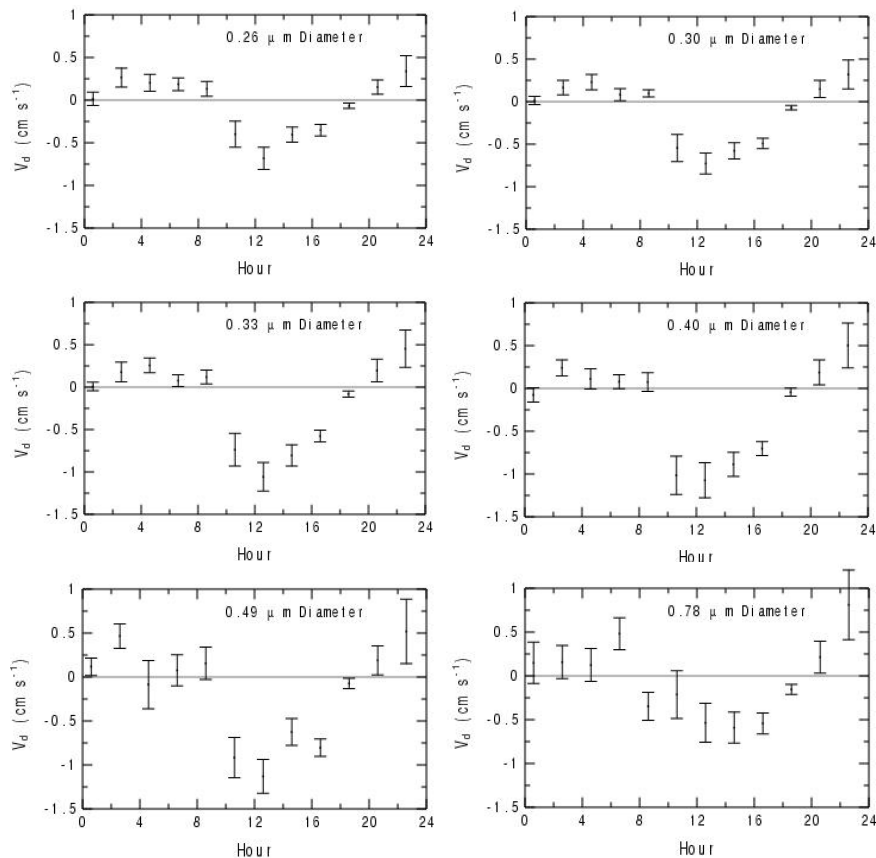


**Fig. 1.** Diurnal variation of aerosol deposition velocity for six particle diameters as measured during BEARPEX 2007 (negative is downward). No corrections have been applied to these data. Bars indicate  $\pm$  one data standard error for values recorded during that two hour period.

[Title Page](#)[Abstract](#)[Introduction](#)[Conclusions](#)[References](#)[Tables](#)[Figures](#)[◀](#)[▶](#)[◀](#)[▶](#)[Back](#)[Close](#)[Full Screen / Esc](#)[Printer-friendly Version](#)[Interactive Discussion](#)

Size-dependent  
aerosol deposition  
velocities

R. J. Vong et al.

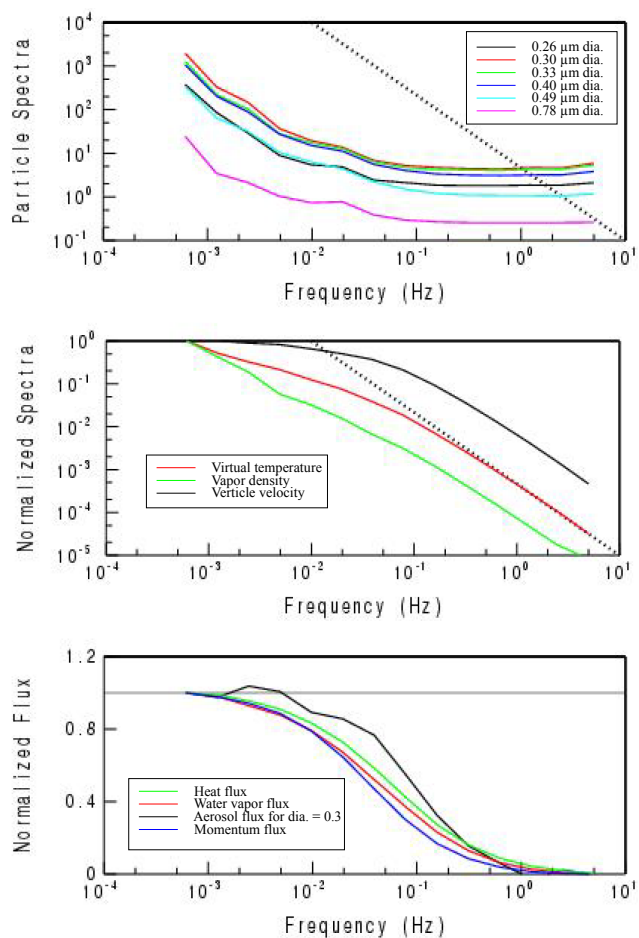
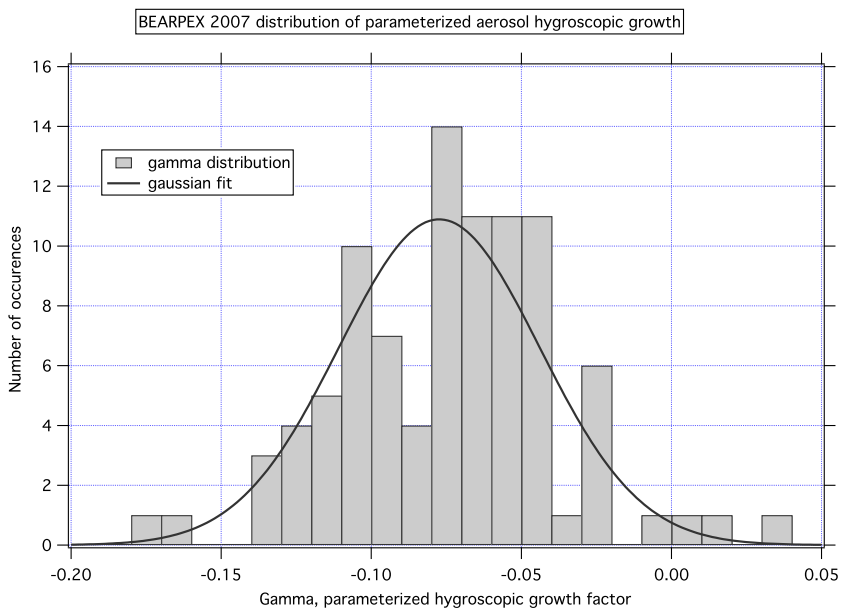


**Fig. 2.** Spectra and co-spectra for the indicated variables from 70 daytime periods during BEARPEX.

[Title Page](#)[Abstract](#)[Introduction](#)[Conclusions](#)[References](#)[Tables](#)[Figures](#)[◀](#)[▶](#)[◀](#)[▶](#)[Back](#)[Close](#)[Full Screen / Esc](#)[Printer-friendly Version](#)[Interactive Discussion](#)

**Size-dependent  
aerosol deposition  
velocities**

R. J. Vong et al.

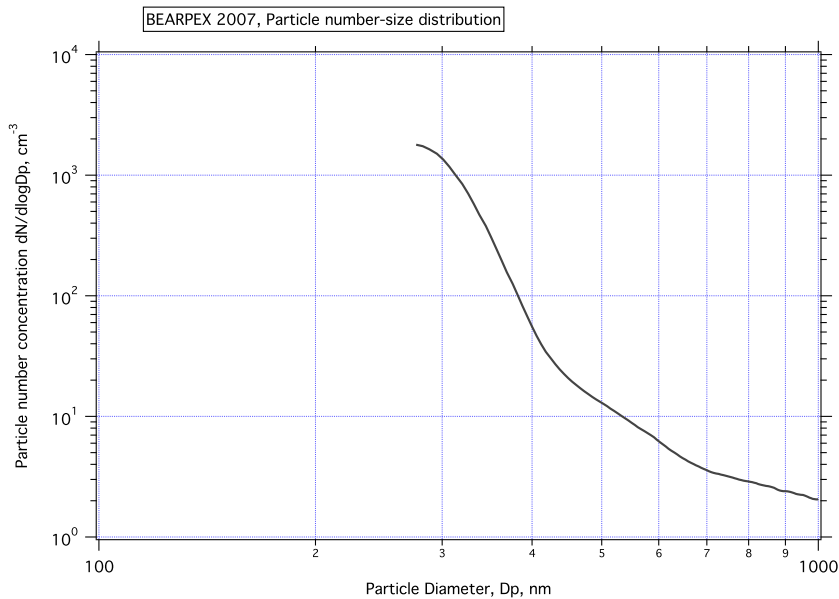


**Fig. 3.** Measured aerosol hygroscopic growth parameter (here as  $-\gamma$ ) during BEARPEX 2007. The plot shows frequency of occurrence and a Gaussian fit to the distribution.

[Title Page](#)[Abstract](#)[Introduction](#)[Conclusions](#)[References](#)[Tables](#)[Figures](#)[◀](#)[▶](#)[◀](#)[▶](#)[Back](#)[Close](#)[Full Screen / Esc](#)[Printer-friendly Version](#)[Interactive Discussion](#)

**Size-dependent  
aerosol deposition  
velocities**

R. J. Vong et al.

**Fig. 4.** Mean aerosol size distribution from the OPC during BEARPEX'07.[Title Page](#)[Abstract](#)[Introduction](#)[Conclusions](#)[References](#)[Tables](#)[Figures](#)[◀](#)[▶](#)[◀](#)[▶](#)[Back](#)[Close](#)[Full Screen / Esc](#)[Printer-friendly Version](#)[Interactive Discussion](#)

**Size-dependent  
aerosol deposition  
velocities**

R. J. Vong et al.

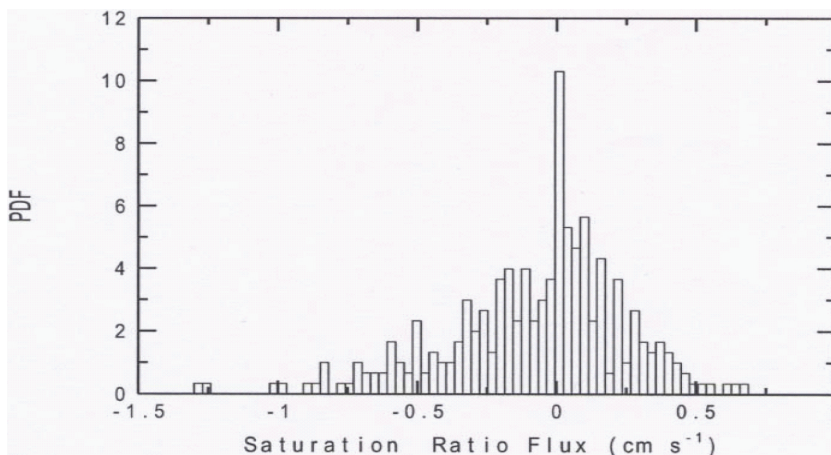


**Fig. 5.** Frequency of occurrence for saturation ratio fluxes during BEARPEX'07 measurements.

[Title Page](#)[Abstract](#)[Introduction](#)[Conclusions](#)[References](#)[Tables](#)[Figures](#)[◀](#)[▶](#)[◀](#)[▶](#)[Back](#)[Close](#)[Full Screen / Esc](#)[Printer-friendly Version](#)[Interactive Discussion](#)

Size-dependent  
aerosol deposition  
velocities

R. J. Vong et al.

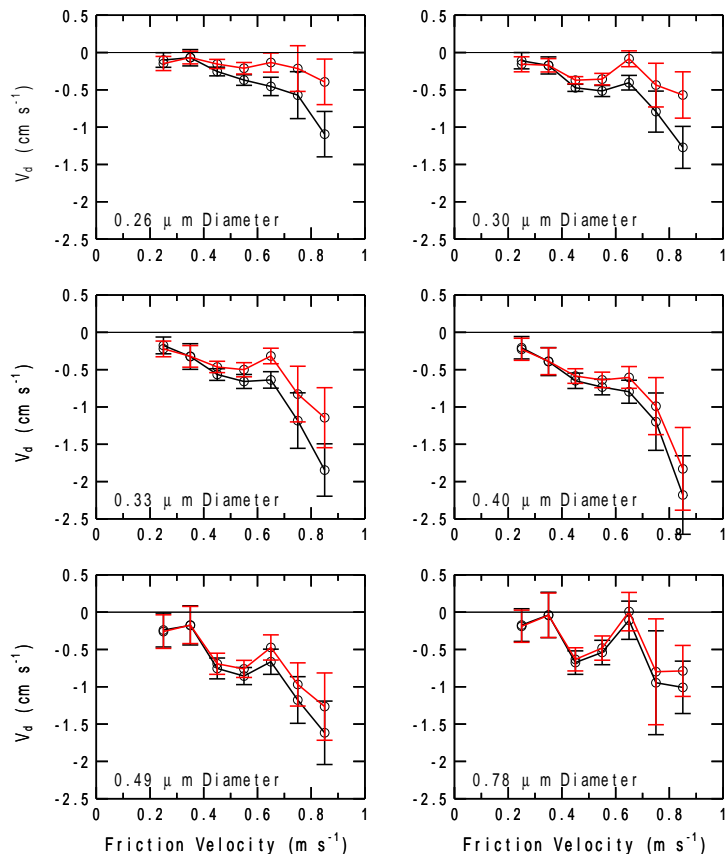


**Fig. 6.** Aerosol deposition velocities (daytime measured values, WPL corrected) versus friction velocity, both with (red) and without (black) the hygroscopic growth correction. Bars indicate  $\pm$ one data standard error.

[Title Page](#)[Abstract](#)[Introduction](#)[Conclusions](#)[References](#)[Tables](#)[Figures](#)[◀](#)[▶](#)[◀](#)[▶](#)[Back](#)[Close](#)[Full Screen / Esc](#)[Printer-friendly Version](#)[Interactive Discussion](#)

Size-dependent  
aerosol deposition  
velocities

R. J. Vong et al.

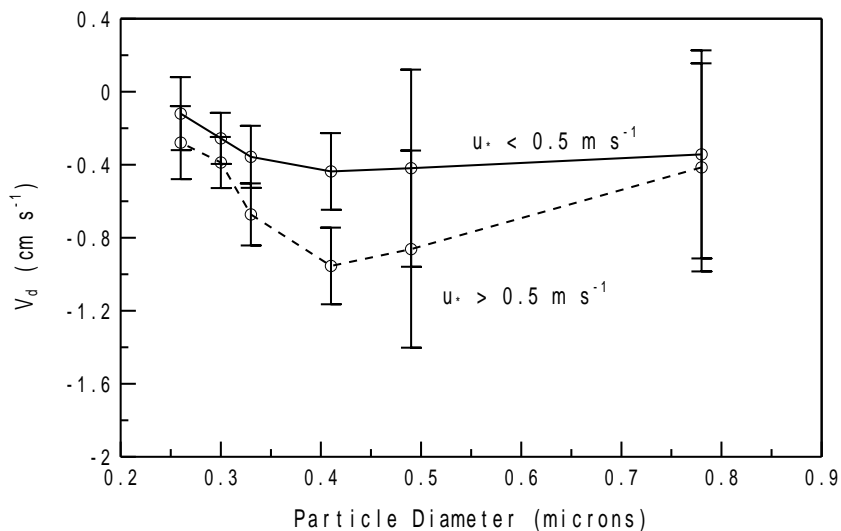


**Fig. 7.** Size dependence of aerosol deposition velocity (corrected for hygroscopic growth and WPL). Bars indicate  $\pm$  the average counting error for single 30 min fluxes.

[Title Page](#)[Abstract](#)[Introduction](#)[Conclusions](#)[References](#)[Tables](#)[Figures](#)[◀](#)[▶](#)[◀](#)[▶](#)[Back](#)[Close](#)[Full Screen / Esc](#)[Printer-friendly Version](#)[Interactive Discussion](#)